JVI Journals.ASM.org

# Syntaxin 5-Dependent Retrograde Transport to the *trans*-Golgi Network Is Required for Adeno-Associated Virus Transduction

**Mathieu E. Nonnenmacher,[a] Jean-Christophe Cintrat,[b] Daniel Gillet,[c] Thomas Weber[a]**

Cardiovascular Research Center, Icahn School of Medicine at Mount Sinai, New York, New York, USA[a]; CEA, iBiTec-S/SCBM, CEA-Saclay, LabEx LERMIT, Gif-sur-Yvette, France[b]; CEA, iBiTec-S/SIMOPRO, CEA-Saclay, LabEx LERMIT, Gif-sur-Yvette, France[c]

## ABSTRACT

**Intracellular transport of recombinant adeno-associated virus (AAV) is still incompletely understood. In particular, the trafficking steps preceding the release of incoming AAV particles from the endosomal system into the cytoplasm, allowing subsequent nuclear import and the initiation of gene expression, remain to be elucidated fully. Others and we previously showed that a significant proportion of viral particles are transported to the Golgi apparatus and that Golgi apparatus disruption caused by the drug brefeldin A efficiently blocks AAV serotype 2 (AAV2) transduction. However, because brefeldin A is known to exert pleiotropic effects on the entire endosomal system, the functional relevance of transport to the Golgi apparatus for AAV transduction remains to be established definitively. Here, we show that AAV2 trafficking toward the *trans*-Golgi network (TGN) and the Golgi apparatus correlates with transduction efficiency and relies on a nonclassical retrograde transport pathway that is independent of the retromer complex, late endosomes, and recycling endosomes. AAV2 transduction is unaffected by the knockdown of syntaxins 6 and 16, which are two major effectors in the retrograde transport of both exogenous and endogenous cargo. On the other hand, inhibition of syntaxin 5 function by small interfering RNA silencing or treatment with cyclized Retro-2 strongly decreases AAV2 transduction and transport to the Golgi apparatus. This inhibition of transduction is observed with several AAV serotypes and a number of primary and immortalized cells. Together, our data strongly suggest that syntaxin 5-mediated retrograde transport to the Golgi apparatus is a broadly conserved feature of AAV trafficking that appears to be independent of the identity of the receptors used for viral attachment.**

## IMPORTANCE

**Gene therapy constitutes a promising approach for the treatment of life-threatening conditions refractory to any other form of remedy. Adeno-associated virus (AAV) vectors are currently being evaluated for the treatment of diseases such as Duchenne muscular dystrophy, hemophilia, heart failure, Parkinson's disease, and others. Despite their promise as gene delivery vehicles, a better understanding of the biology of AAV-based vectors is necessary to improve further their efficacy. AAV vectors must reach the nucleus in order to deliver their genome, and their intracellular transport is not fully understood. Here, we dissect an important step of the intracellular journey of AAV by showing that retrograde transport of capsids to the *trans*-Golgi network is necessary for gene delivery. We show that the AAV trafficking route differs from that of known Golgi apparatus-targeted cargos, and we raise the possibility that this nonclassical pathway is shared by most AAV variants, regardless of their attachment receptors.**

Due to their intrinsically low immunogenicity, their ability to infect a variety of tissues *in vivo*, and their capacity to confer prolonged transgene expression in postmitotic tissues (1), vectors based on adeno-associated virus (AAV) are among the most promising gene therapy tools. Although these properties make AAV an attractive candidate for many clinical applications, some tissues or cell types are not efficiently transduced by AAV vectors, presumably due to the absence of viral receptors, inefficient intracellular trafficking, or viral uncoating (recently reviewed in reference 2).

AAVs contain a single-stranded DNA genome, and the entire viral replication cycle—second-strand DNA synthesis, replication of viral genomes, and encapsidation—takes place in the nucleus. Therefore, correct trafficking of incoming virions from the plasma membrane toward the nuclear compartment is of crucial importance for viral or therapeutic gene expression. Following the initial attachment to a primary glycoprotein receptor (heparan sulfate proteoglycan for AAV serotype 2 [AAV2], AAV3, and AAV6; sialic acids for AAV1, AAV4, AAV5, and AAV6; and N-linked galactose for AAV9 [2]), viral particles undergo rapid endocytosis. Whereas more than one endocytic mechanism might play a role in AAV transduction (3–7), the most productive endocytosis appears to occur through the clathrin-independent carrier (CLIC)/GPI-anchored-protein-enriched early endosomal compartments (GEEC) pathway, at least for AAV2 in HeLa and HEK293T cells (5). After internalization, the low pH in endosomes (8) and, possibly, the action of endosomal proteases (9) trigger a conformational change in the AAV capsid, exposing the N-terminal domain of the largest capsid protein, VP1, on the capsid surface (10). This so-called VP1 unique region ($VP1_u$) harbors a phospholipase A2

**Received** 2 September 2014 **Accepted** 11 November 2014

**Accepted manuscript posted online** 19 November 2014

**Citation** Nonnenmacher ME, Cintrat J-C, Gillet D, Weber T. 2015. Syntaxin 5-dependent retrograde transport to the *trans*-Golgi network is required for adeno-associated virus transduction. J Virol 89:1673–1687. doi:10.1128/JVI.02520-14.

**Editor:** M. J. Imperiale

Address correspondence to Thomas Weber, thomas.weber@mssm.edu.



doi:10.1128/JVI.02520-14

(PLA2) domain and a bipartite nuclear localization signal, which are sequentially required for escape into the cytoplasm and the nuclear import of intact capsids (11–15). Both the escape into the cytoplasm and the nuclear import have been proposed to be rate limiting because only a small fraction of virions successfully reaches the nucleus, and the majority can instead be observed in a perinuclear vesicular compartment for extended periods (16–18). The precise mechanism of viral trafficking from early endosomal vesicles to the cytoplasm is largely unexplored, with some proposed models involving the early endosomes (EEs)/recycling endosomes (REs) (3, 19, 20) and others involving the late endosomal/lysosomal compartment (8, 19, 21, 22).

Several groups, including ours, have shown that AAV capsids rapidly accumulate in the *trans*-Golgi network (TGN) and the Golgi apparatus proper (5, 23–25), suggesting that AAV takes advantage of the endosome-to-TGN retrograde transport machinery to reach the cytoplasm. Retrograde transport through the endocytic system is a highly regulated and selective process that allows the retrieval of specific proteins or lipids from the plasma membrane and their transport to the TGN, the Golgi apparatus, and, in some cases, the endoplasmic reticulum (ER) (26). Notably, bacterial and plant toxins, such as cholera toxin, Shiga toxin, pertussis toxin, and ricin, hijack this system in order to reach the cytoplasm, where they exert their cytotoxic effects (27, 28). Interestingly, the oncogenic, small, nonenveloped human papillomavirus 16 (HPV16) has also been reported to rely on retrograde transport to reach the TGN and, ultimately, the cytoplasm (29, 30).

Today, on the basis of the identity of intermediate endosomal compartments and the nature of translocated cargo, retrograde transport is typically divided into two principal routes in mammalian cells. The first pathway proceeds sequentially through the EEs and late endosomes (LEs) toward the TGN (EE-LE-TGN) and is used, for instance, by the cation-independent mannose-6-phosphate receptor (Ci-MPR) (31), the TGN-resident protease furin (32), and HPV16 pseudovirions (29). This pathway is regulated by the small GTPase Rab9 and by the tSNARE (target membrane soluble *N*-ethylmaleimide-sensitive factor [NSF] attachment protein receptor) syntaxin 10 (STX10) (33). Shiga toxin B is a model cargo of the second pathway, which allows direct transport from EEs to the TGN or, in some instances, successive transport via recycling endosomes (EE-RE-TGN) (34). Notably, this route is used by cholera toxin B. This conduit depends specifically on the action of Rab11 and STX6 (33, 35, 36). Other elements, such as the Vps26/29/35 retromer complex and the tSNAREs STX5 and STX16, are essential for both pathways (26).

Here, we investigate the relevance of these retrograde transport pathways to the Golgi apparatus in AAV-mediated transduction. Using a recently developed Golgi apparatus-targeting drug and small interfering RNA (siRNA)-mediated knockdown of specific transport proteins, we show that transport to the Golgi apparatus is indispensable for AAV transduction, and we present evidence that AAV uses an as of yet poorly described, alternative retrograde transport mechanism that requires STX5. This route functions independently of well-known effectors of the classical LE-TGN and EE-RE-TGN pathways, which is consistent with productive AAV infection proceeding through a noncanonical endosome-to-TGN retrograde transport pathway.

## MATERIALS AND METHODS

**Cell lines.** HEK293T, HeLa, NIH 3T3, and Huh7 cells (ATCC, Manassas, VA) were maintained in Dulbecco modified Eagle medium (DMEM) with 10% fetal bovine serum (FBS) (Sigma, St. Louis) and antibiotics. Human coronary artery endothelial cells (HCAECs) were purchased from Lonza and cultured in EGM2 MV medium (Lonza, Basel, Switzerland). Adult rat cardiomyocyte isolation and transduction were performed as previously described (37). Human umbilical vein endothelial cells (HUVECs) were obtained from Promocell and cultured in EGM2 MV medium (Lonza, Basel, Switzerland).

**Plasmid and siRNA transfection.** Sequences encoding human Rab7, Rab9, and Rab11 were obtained by reverse transcription-PCR (RT-PCR) from HeLa cell total RNA using SuperScript III enzyme (Life Technologies) with an oligo(dT) primer. PCR was performed with an Expand high-fidelity PCR system (Roche) using primers incorporating an EcoRI site in the 5′ end and a SalI site in the 3′ end of the amplicon. PCR products were cloned between the EcoRI and SalI sites of the pEGFP-C1 plasmid (Clontech) or the equivalent pmCherry-C1 plasmid to obtain enhanced green fluorescent protein (EGFP)-Rab or mCherry-Rab fusion proteins. Dominant negative mutations (Rab7 T22N, Rab9 S21N, and Rab11 S25N) were obtained using a QuikChange mutagenesis method (Stratagene) or 2-step overlap PCR using Phusion polymerase (New England BioLabs). Plasmids were transfected into HEK293T cells using calcium phosphate precipitation and routinely yielded ~75% transfection, estimated by microscopic observation of fluorescent cells. RNA interference was performed using Silencer Select siRNA or stealth siRNA (Life Technologies). HeLa cells were seeded in 24-well plates in antibiotic-free DMEM with 10% FBS and transfected with a mixture of 10 pmol siRNA and 1 μl Lipofectamine 2000 (Life Technologies) in 100 μl of Opti-MEM medium. The medium was changed after 16 h, and the cells were incubated for another 24 h before viral transduction, RNA extraction, or immunoblotting. For immunofluorescence, cells were trypsinized on the day after siRNA transfection and replated at a low density on 12-mm glass coverslips in 24-well plates. For ER fluorescent labeling, HeLa cells grown on glass coverslips were transfected with a tandem-dTomato-KDEL plasmid (a kind gift from Kirsten Sadler Edepli, Icahn School of Medicine at Mount Sinai) using 200 ng of plasmid and 1 μl Lipofectamine 2000 per well in antibiotic-free DMEM.

**Recombinant virus production.** Recombinant AAVs were produced using the two-plasmid method and pDG or pDP vectors harboring CAP proteins of AAV serotype 1, 2, 3, 4, 5, 6, 8, or 9 (38, 39). HEK293T cells were cotransfected with pDG/pDP vectors and pTR-luciferase or ds-mCherry vectors (which have been previously described [5]), and virus was purified from cell lysates on iodixanol gradients (5, 40). Viral titers were determined by real-time PCR with primers specific for luciferase (Luc) or simian virus 40 (SV40) poly(A). Adenovirus type 5 (Ad5) carrying an EGFP transgene was kindly provided by Lifan Liang (Icahn School of Medicine at Mount Sinai, New York, NY).

**Transduction assays.** For endpoint transduction studies, cells were pretreated with chemical inhibitors for 30 min at 37°C and infected with AAV-luciferase at a multiplicity of infection (MOI) of 100, 1,000, or 10,000 viral genomes (vg) per cell or with Ad5-EGFP at an MOI of 10,000 particles per cell. Cells were incubated with the virus overnight in the presence of the inhibitors. For luciferase activity measurement, cells were lysed in Tris-buffered saline containing 1% NP-40 and 2 mM EDTA, and luciferase activity was measured using a Promega luciferase assay system on a Synergy 2 plate reader (BioTek). Luciferase counts were normalized to the total protein content measured using a bicinchoninic acid assay (Thermo Scientific).

For drug addition kinetics experiments, HeLa cells were cooled down on ice for 15 min and virus was added for 30 more minutes to allow attachment. Unbound virus was removed by 4 washes in ice-cold medium. After the final wash, prewarmed medium was added and the cells were immediately transferred to 37°C. Drugs were then added at various time points, and the luciferase activity of lysates was measured at 24 h

postwarming. The following inhibitors were used in this study: brefeldin A (BFA), golgicide A, and bafilomycin A1 (all from Sigma-Aldrich) and Retro-2 (EMD Millipore). Retro-2c and Retro-2.1 were synthesized in-house (41, 42). The effect of various drugs on cell viability was measured using the CellTiter-Glo assay (Promega).

**AAV endocytosis assay.** AAV2-luciferase was added to HeLa cells for 1 h at 37°C at an MOI of 10,000, and noninternalized virus was removed by adding heparin at a final concentration of 100 μg/ml, as previously described (5). After 30 min incubation with heparin, cells were washed thoroughly and trypsinized to ensure complete extracellular virus removal. Low-molecular-weight DNA was then extracted using Zyppy plasmid miniprep columns (Zymo Research, Irvine, CA), and viral DNA was quantified by real-time PCR using primers specific for the luciferase sequence.

**Immunofluorescence and immunoblotting.** For experiments involving AAV2 subcellular localization, virus was added at an MOI of 10,000 vg/cell for 1 h at 37°C, and then extracellular virus was removed by adding 100 μg/ml heparin directly to the medium and the cells were further incubated until the time points indicated below. This step was necessary to synchronize incoming virions along the trafficking pathway. In all experiments, cells plated on 12-mm glass coverslips were fixed in 4% paraformaldehyde for 15 min at room temperature, permeabilized in 0.2% Triton X-100, and blocked for 1 h in immunofluorescence (IFM) buffer (20 mM Tris [pH 7.5], 137 mM NaCl, 3 mM KCl, 1.5 mM $MgCl_2$, 5 mg/ml bovine serum albumin, 0.05% Tween). Cells were incubated overnight at 4°C with primary antibodies diluted in IFM buffer, washed 3 times for 5 min each time in IFM buffer, and incubated for 1 h with fluorescently labeled secondary antibodies. Nuclei were counterstained with DAPI (4′,6-diamidino-2-phenylindole), and cells were mounted in Mowiol mounting medium. Images were acquired with a Leica SP5 laser scanning confocal microscope at the Icahn School of Medicine at Mount Sinai Microscopy Shared Resource Facility and processed using the Photoshop program for illustrations (contrast and brightness were uniformly adjusted without gamma correction). Colocalization analysis was performed on unmodified confocal microscopy images using the image calculator function of ImageJ software by setting the pixel intensity threshold at 100. The total colocalized pixel intensity was then calculated using the histogram function of ImageJ software. The primary antibodies used in this study were mouse anti-AAV2 capsid A20 (catalog number 03-61055; American Research Products), rabbit anti-giantin (catalog number ab24586; Abcam), rabbit anti-golgin-97 (catalog number D8P2K; Cell Signaling Technologies), mouse anti-Ci-MPR (catalog number MAI-066; Pierce), rabbit anti-TGN38/46 (catalog number NBP1-49643; Novus), goat anti-Vps35 (catalog number A20090; Genway), rabbit anti-Rab7 (catalog number D95F2; Cell Signaling Technologies), rabbit anti-Rab9 (catalog number D52G8; Cell Signaling Technologies), rabbit anti-Rab11 (catalog number D4F5; Cell Signaling Technologies), rabbit anti-STX5 (catalog number 110053; Synaptic Systems), rabbit anti-STX6 (catalog number C34B2; Cell Signaling Technologies), and rabbit anti-GAPDH (anti-glyceraldehyde-3-phosphate dehydrogenase; catalog number G9545; Sigma).

## RESULTS

**Transport of AAV2 to the Golgi apparatus is required for transduction.** Others and we have observed that a large proportion of AAV2 capsids accumulate in the Golgi apparatus shortly after virus uptake (5, 23–25). Furthermore, AAV2 transduction is dramatically reduced following treatment with the fungal metabolite brefeldin A (BFA) (5, 8), a drug known to trigger the coalescence of the Golgi apparatus with the ER and to inhibit protein secretion (43). However, BFA exerts pleiotropic functions on trafficking, notably, by inducing the tubulation of early endosomes and by blocking early-to-late endosome fusion (44, 45). Hence, we decided to use golgicide A, a highly specific inhibitor of the Golgi apparatus Arf1 guanine nucleotide exchange factor GBF1 (46) to confirm the importance of transport to the Golgi apparatus for AAV transduction. Golgicide A has been shown to disrupt the Golgi apparatus and to block retrograde transport of Shiga toxin between the early endosomes and the TGN (46, 47). We infected HeLa or HEK293T cells with an AAV2 vector containing a luciferase expression cassette (AAV2-Luc) either in the absence or in the presence of increasing concentrations of BFA or golgicide A. Luciferase activity was measured at 24 h postinfection. Both compounds showed a strong inhibition of AAV2 transduction in both cell lines (Fig. 1A), suggesting that transport to the Golgi apparatus is a prerequisite for successful AAV2 transduction. Both cells treated with BFA and cells treated with golgicide A showed a significant, 4- to 5-fold reduction of viability at 24 h posttreatment (data not shown), but this effect clearly did not account to a significant extent for the dramatic block of AAV transduction, which was reduced by 2 orders of magnitude. Addition of the drugs at different times postinfection revealed very similar loss-of-inhibition kinetics, with half-lives ($t_{1/2}$) of approximately 2.5 h (Fig. 1B). These results (i) indicate that loss of transduction is not a result of cytotoxicity and (ii) are consistent with both compounds interfering with the same transport step.

In agreement with this interpretation, confocal microscopy observation of HeLa cells 3 h after infection with AAV2 showed that BFA and golgicide A exerted a dramatic effect on both Golgi apparatus morphology and the subcellular localization of AAV2 capsids. Whereas control cells showed a high extent of colocalization between AAV2 capsids and the Golgi apparatus marker giantin (Fig. 1C, left), BFA and golgicide A treatment induced a complete dispersal of the Golgi apparatus and prevented the transport of AAV2 capsids toward the perinuclear region (Fig. 1C).

Compared to HeLa cells, NIH 3T3 cells are fairly refractory to AAV2 infection, despite a similar rate of endocytosis (48). In agreement with these results, AAV2 infection of NIH 3T3 cells resulted in an approximately 15-fold lower level of transgene expression compared to that for HeLa cells (Fig. 1D). Interestingly, in NIH 3T3 cells, few, if any, viral capsids accumulated in the Golgi apparatus (Fig. 1E), confirming earlier reports that the poor transducibility of NIH 3T3 cells is the result of trafficking along a nonproductive route (48, 49). This implies that AAV Golgi apparatus accumulation strongly correlates with transduction efficiency and that impaired retrograde transport may account for the low transduction efficiencies of certain cell types.

Previous reports demonstrated that endosomal acidification is required for AAV transduction (8, 23). It has also been shown that retrograde transport of cellular proteins to the ER can be inhibited with bafilomycin A1 (50). These reports open the possibility that endosome acidification is necessary for retrograde transport of AAV. However, whereas exposure of HeLa cells to the endosomal $H^+$-ATPase inhibitor bafilomycin A1 resulted in a drastic inhibition of transduction (Fig. 1F), the accumulation of AAV2 capsids in the Golgi compartment was unaffected (Fig. 1G). Furthermore, the comparative kinetics of bafilomycin A1 and golgicide A addition indicate that the requirement for endosomal acidification ($t_{1/2}$, ~1.5 h) precedes transport to the Golgi apparatus ($t_{1/2}$, ~2.5 h).

**AAV2 virions do not accumulate in the ER.** With the exception of HPV16, all known pathogens or toxins depending on retrograde transport to the Golgi apparatus, including Shiga toxin, cholera toxin, ricin, or SV40, must be transported to the endoplas-

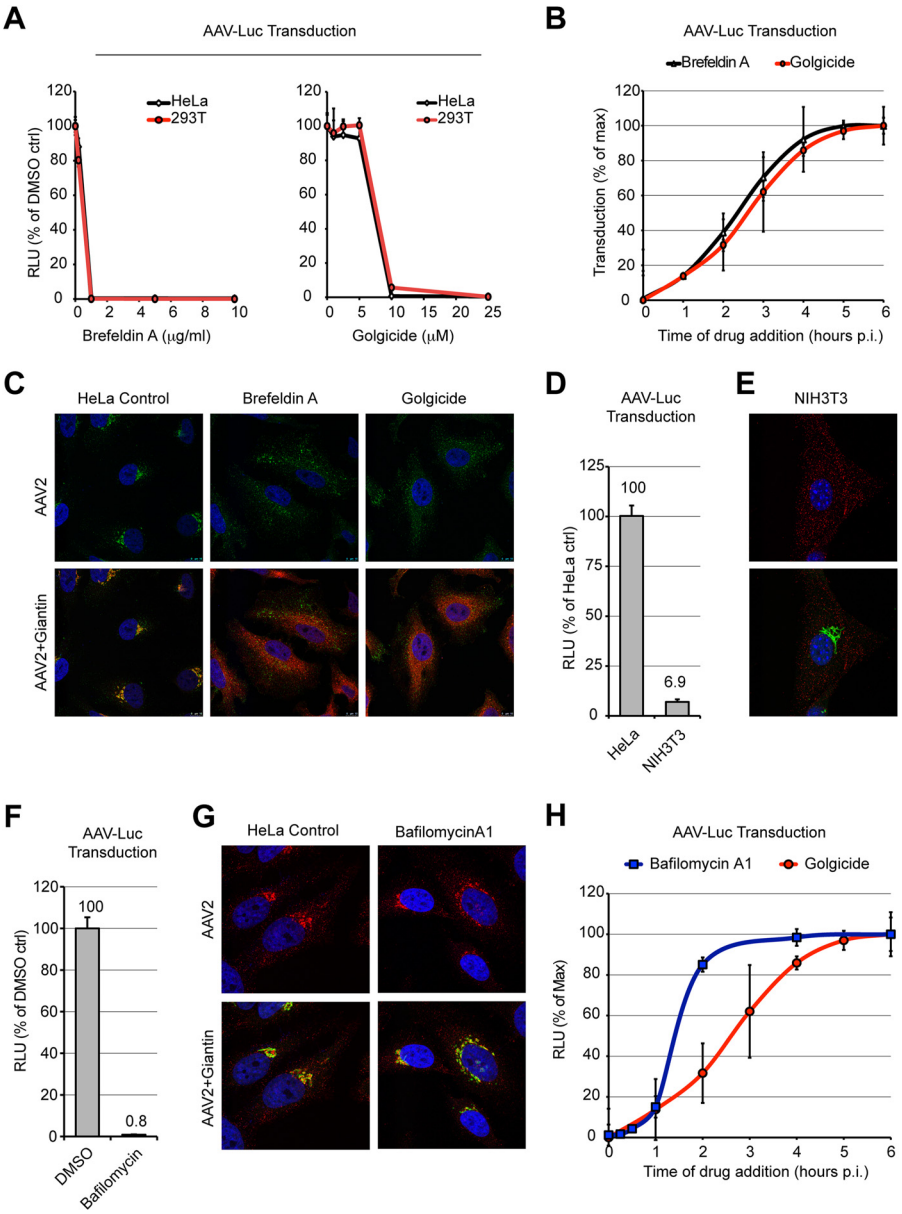


**FIG 1** Inhibition of AAV2 transduction by Golgi apparatus-targeting drugs. (A) HeLa or HEK293T cells pretreated with various concentrations of brefeldin A or golgicide A were infected with AAV2-Luc at an MOI of 10,000. Luciferase activity was measured at 24 h postinfection and normalized to that for the dimethyl sulfoxide (DMSO)-treated controls (ctrl). RLU, relative light units. (B) Kinetics of drug addition. HeLa cells were allowed to bind AAV2-Luc on ice for 30 min, washed, and transferred to 37°C. Drugs were added at different times postwarming, and luciferase activity was measured at 24 h postwarming. Luciferase reads were normalized to the maximum plateau value rather than the value for the dimethyl sulfoxide-treated controls in order to compensate for the long-term cytotoxicity of brefeldin A and golgicide, which both reduce cell viability by 60 to 80% after 24 h of incubation. p.i., postinfection. (C) Subcellular localization of AAV2 capsids (green) and the Golgi apparatus marker giantin (red) at 3 h postinfection in cells treated by Golgi apparatus-targeting drugs. (D) AAV2-Luc transduction of poorly permissive NIH 3T3 cells compared to that of permissive HeLa cells. Identical numbers of cells were infected to allow direct comparison. (E) Subcellular localization of AAV2 capsids (red) and giantin (green) in poorly permissive NIH 3T3 cells at 3 h postinfection. (F) AAV2-Luc transduction of HeLa cells treated with bafilomycin A1. Values represent luciferase activity normalized to that for the dimethyl sulfoxide-treated controls. (G) Subcellular localization of AAV2 capsids (red) and giantin (green) in HeLa cells treated with bafilomycin A1. (H) Comparison of the addition kinetics of bafilomycin A1 and golgicide. Drugs were added at various times following AAV2-Luc infection. Luciferase values were normalized to the maximum plateau values, as described in the legend to panel B.

mic reticulum to exert their effects. Reportedly, SV40 and the bacterial and plant toxins take advantage of the misfolded protein response machinery, the molecular chaperone BiP, and the Sec61 translocon (51, 52) to be retrotranslocated into the cytoplasm. Hence, we asked whether AAV capsids could reach the ER during their retrograde journey. Immunostaining of AAV2 capsids at various times postentry showed no appreciable colocalization with the fluorescent ER marker protein ER-tdTmt (Fig. 2A). In contrast, Golgi apparatus accumulation of capsids was evident as early as 1 h postentry (Fig. 2A). Quantification of colocalization from multiple microscopic fields showed that the percentage of AAV2 capsids that colocalized with the TGN marker golgin-97 gradually

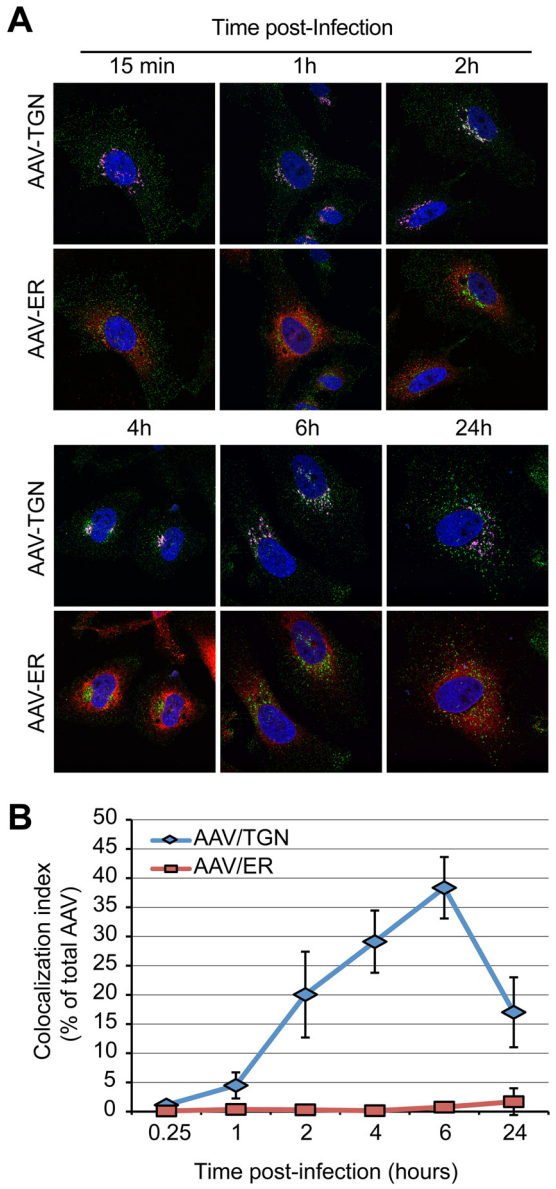


**FIG 2** Lack of evidence for AAV ER transport. (A) HeLa cells transfected with the ER marker plasmid pER-dTmT (red) were infected with AAV2-Luc at an MOI of 10,000 and fixed at various times postinfection. Cells were immunostained with an anti-golgin-97 antibody (purple) and an anti-AAV2 capsid antibody (green). Cells were imaged by confocal microscopy. (B) Index of colocalization of AAV2 capsids with TGN or ER, expressed as the percentage of green pixels (AAV2 capsids) colocalized with TGN (purple) or ER (red) pixels. Numbers represent the mean ± SD from triplicate experiments.

increased over time and reached a maximum of 40% at 6 h postentry. AAV2 colocalization with the ER, on the other hand, remained at the background level at all time points (Fig. 2B). Although this does not formally rule out the requirement for transport of AAV2 to the ER for transduction, these data are most easily explained by a model in which AAV2 escapes into the cytoplasm from the TGN or the Golgi apparatus. Interestingly, the extent of AAV2/TGN colocalization was significantly reduced at 24 h postentry, raising the possibility that a fraction of capsids successfully escaped the TGN at that time point (Fig. 2B).

**Retrograde transport of AAV does not depend on the retromer complex or EE-LE-TGN or EE-RE-TGN transport.** We sought to characterize further the retrograde transport pathway used by AAV capsids by studying the involvement of essential components of the canonical EE-LE-TGN pathway or the EE-RE-TGN pathway. First, we transfected HeLa cells with small interfering RNAs (siRNAs) that target the retromer complex component Vps35, which resulted in efficient knockdown, as measured by immunoblotting (Fig. 3A). As expected from previous studies (53), retromer depletion induced a strong dispersal of the cation-independent mannose-6-phosphate receptor (Ci-MPR), the prototypical cargo of LE-dependent retrograde transport, showing that the LE-TGN pathway was functionally disrupted (Fig. 3B). In contrast, Vps35 knockdown had no negative effect on transduction by the AAV2-luciferase vector, regardless of the multiplicity of infection (Fig. 3C). This observation was intriguing because retromer is an essential component of LE-TGN transport, and a previous study suggested that AAV can, in a dose-dependent fashion, traffic through both the late and the recycling endosomal compartments (19). To address this apparent discrepancy, we further tested the involvement of the late endosomal compartment by knocking down Rab9, a highly specific effector of LE-TGN transport (31), with three independent siRNAs. All three siRNAs that we tested showed effective knockdown, ranging from 80% to 95%, as shown by Western blotting (Fig. 4A). Similar to the findings for cells treated with Vps35 siRNA, HeLa cells transfected with Rab9 siRNA showed a strong dispersal of the Ci-MPR, confirming the functional disruption of LE-TGN transport (Fig. 4B). However, when siRNA-treated cells were infected with AAV2-luciferase at an MOI of 100, 1,000, or 10,000 viral genomes (vg) per cell, none of the Rab9 siRNAs showed any inhibition of AAV2-luciferase transduction (Fig. 4C). On the contrary, all three siRNAs showed a trend toward an increase in AAV transduction (Fig. 4C). Interestingly, the lack of inhibition of transduction was observable independently of the MOI used, which indicates that late endosomes are not required for AAV transduction irrespective of the viral dose, as was previously reported (17). In further support of this model, we observed no inhibition of transduction in HEK293T cells that were transfected with a dominant negative mutant of Rab9 (Fig. 4D). A similar set of experiments was performed to evaluate the role of Rab7, another essential factor of late endosome trafficking and biogenesis (54). Two out of three siRNAs effectively reduced Rab7 protein expression (Fig. 4E). Rab7 depletion efficiently blocked retrograde trafficking of Ci-MPR (Fig. 4F), but none of the siRNAs was able to inhibit AAV2-luciferase transduction at a high, medium, or low MOI (Fig. 4G). Consistently, overexpression of a Rab7 dominant negative mutant in HEK293T cells had no significant effect on AAV2 transduction (Fig. 4H).

Having excluded the possibility of any involvement of late endosomes in retrograde trafficking of AAV2, we investigated a potential role of recycling endosomes in AAV2 transduction. We used a set of three siRNAs to knock down Rab11 expression. Each siRNA induced a robust silencing of endogenous Rab11 (Fig. 5A). Consistent with the central role of Rab11 in RE-TGN transport, cells transfected with Rab11 siRNA1 showed an obvious mislocalization of TGN46, a well-characterized cargo of the RE-TGN retrograde pathway (35) (Fig. 5B). Silencing of Rab11 by any of the three siRNAs did not significantly inhibit AAV2 transduction, irrespective of the MOI (Fig. 5C). One of the siRNAs (siRNA1) induced a 2.5- to 3-fold increase in luciferase expression, which,

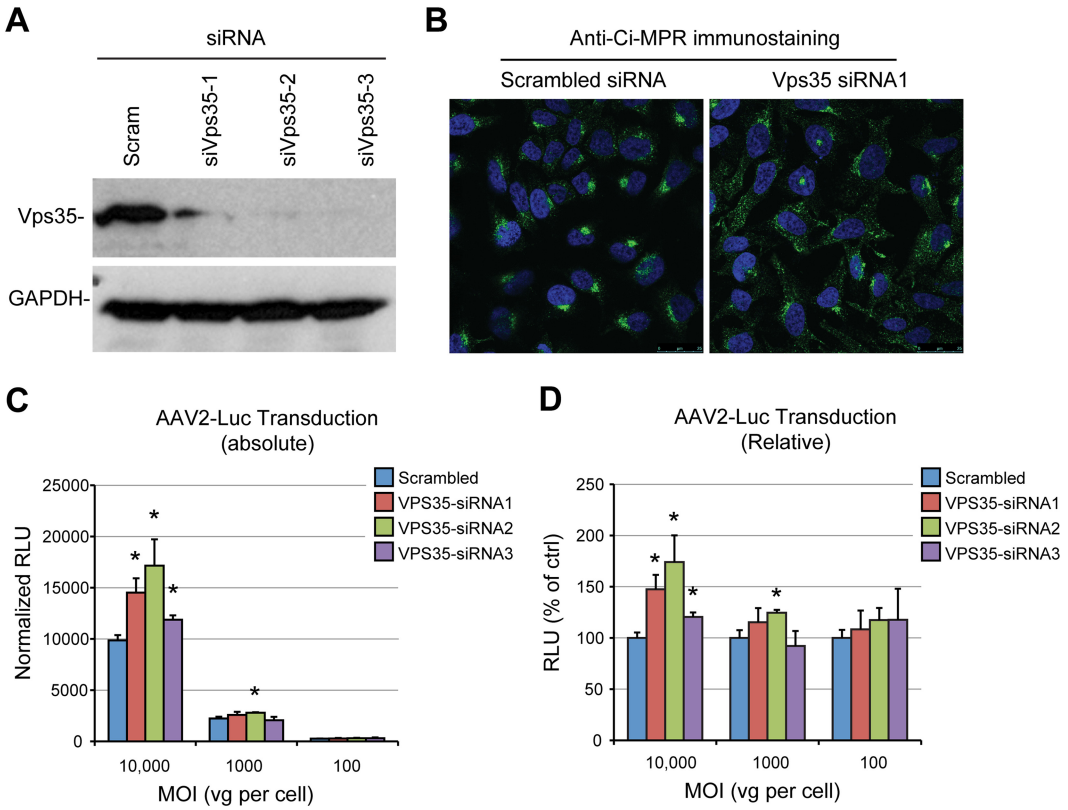


**FIG 3** AAV transduction is independent of retromer function. (A) Validation of siRNA-mediated knockdown of Vps35 by immunoblotting. HeLa cell lysates were harvested 48 h after siRNA transfection. Scram, scrambled; siVps35-1 to siVps35-3, three different siRNAs against Vps35. (B) Steady-state localization of Ci-MPR in HeLa cells transfected with Vps35 siRNA. Cells were fixed at 48 h posttransfection, stained with an anti-Ci-MPR antibody, and analyzed by confocal microscopy. (C) AAV2-Luc transduction of HeLa cells treated with Vps35 siRNAs. Cells were infected at various MOIs (10,000, 1,000, or 100 vg/cell) 48 h after siRNA transfection. Values represent absolute luciferase activity normalized to the protein content. Data represent the mean ± SD from triplicate experiments. (D) Relative transduction values normalized to the values for cells transfected with scrambled siRNA. *, $P < 0.05$.

given the lack of stimulation by siRNA2 and siRNA3, most likely is a result of an off-target effect. Consistent with the Rab11 knockdown experiments, transfection of HEK293T cells with a dominant negative mutant of Rab11 did not inhibit AAV2 transduction (Fig. 5D). Overall, our data unambiguously demonstrate that retrograde trafficking of AAV2 does not rely on the retromer complex, late endosomes, or recycling endosomes, at least in HeLa cells. Strikingly, silencing of Vps35, Rab9, or Rab11 also had no effect on transduction by AAV1, a serotype relying on sialic acid instead of heparan sulfate proteoglycans for cell attachment (data not shown). This suggests that different AAV serotypes can converge to a similar retrograde trafficking pathway irrespective of their attachment receptors.

**Role of Golgi apparatus-resident syntaxins in AAV2 transport.** SNAREs (soluble NSF attachment protein receptors) are key determinants in the specificity of intracellular vesicular trafficking (55, 56) and represent the minimal machinery for vesicular membrane fusion (57). SNARE proteins can be divided into two groups, so-called tSNAREs, which reside on a target membrane (e.g., the plasma membrane), and so-called vSNAREs which reside in a vesicular membrane (e.g., synaptic vesicles). Each transport step in a cell is defined by a specific, cognate pair of tSNAREs and vSNAREs (55, 56).

Having established that AAV trafficking was relying on a noncanonical retrograde transport pathway that is independent from late or recycling endosome function, we investigated the role of major Golgi apparatus-resident tSNARE proteins in AAV transduction. We focused our attention on STXs 5, 6, and 16 because these SNAREs have previously been shown to be involved in retrograde trafficking of multiple endogenous and exogenous cargos (26). siRNA knockdown of each STX was effective, as measured by Western blotting (Fig. 6A and B) or quantitative RT-PCR (qRT-PCR) (Fig. 6C). Localization of the TGN marker TGN46 was strongly disturbed following knockdown of STX5, STX6, and STX16 (Fig. 6D, top). This is in agreement with the findings of previous studies indicating that all three proteins are essential for the EE-RE-TGN pathway (36, 58). As previously reported (33), depletion of STX16 induced a strong relocalization of the Ci-MPR into scattered vesicles (Fig. 6D, bottom), indicating functional inhibition of the LE-TGN pathway. In contrast, STX5 siRNA induced only a moderate dispersal of Ci-MPR, and STX6 siRNA had no visible effect (Fig. 6D, bottom). Silencing of STX5 by siRNA1, -2, and -3 reduced AAV2-Luc transduction by 60%, 60%, and 40%, respectively (Fig. 6A). Overexpression of STX5 in HEK293T cells also resulted in a moderate inhibition of AAV2 transduction, but this effect was likely due to a strong cytotoxic effect (data not shown).

In contrast to STX5 siRNA, STX6 and STX16 siRNAs induced a moderate increase in transduction, which was more obvious at a high MOI (Fig. 6B and C). Remarkably, silencing of STX5 also impaired transduction by AAV1-Luc to a similar extent (65% re-

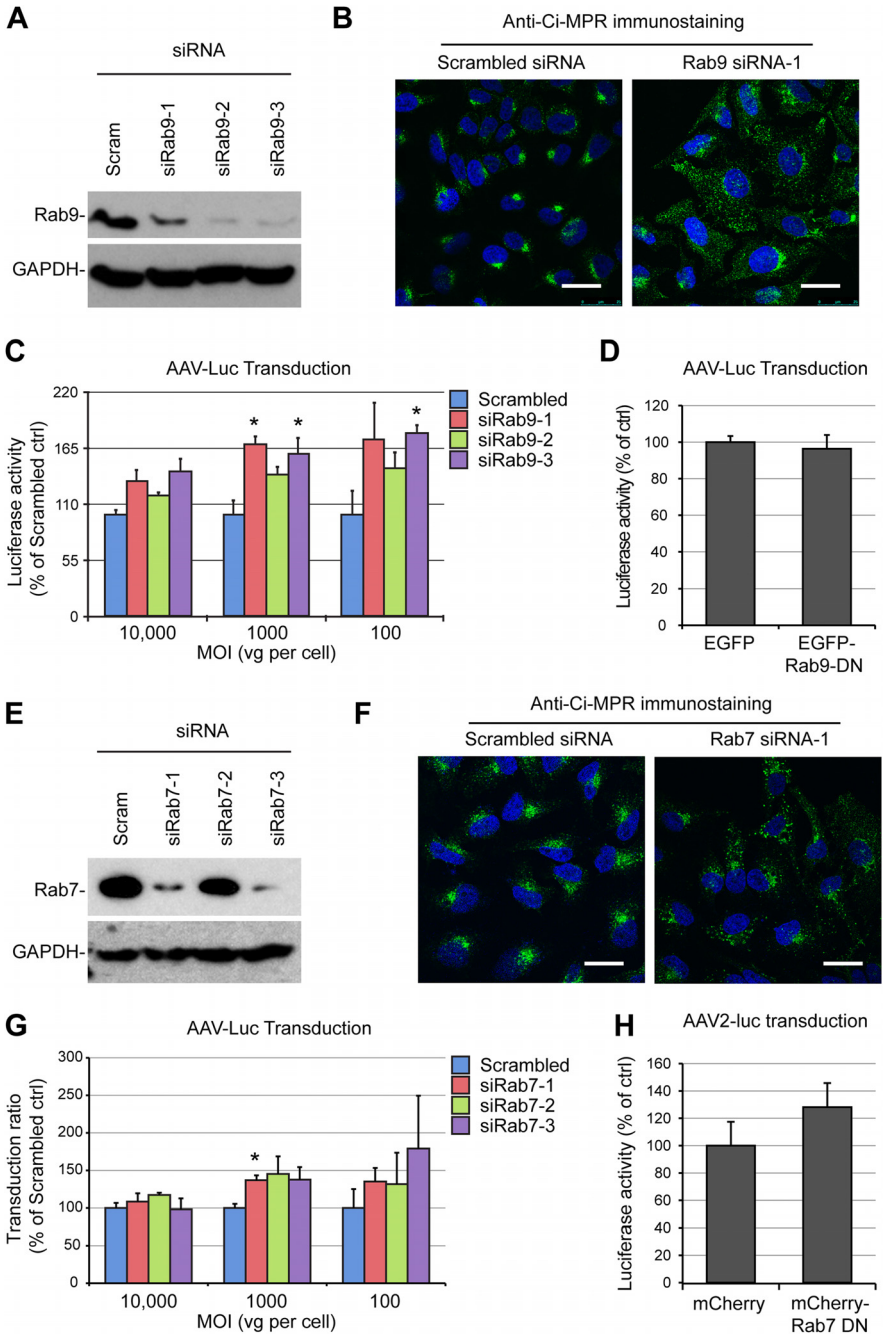


**FIG 4** AAV transduction is independent of late endosome function. (A) Validation of Rab9 knockdown by multiple siRNAs. HeLa cells were transfected with three different siRNAs against Rab9 (siRab9-1 to siRab9-3). Protein extracts were obtained at 48 h posttransfection and analyzed by immunoblotting with a monoclonal Rab9 antibody. (B) Steady-state localization of Ci-MPR in HeLa cells treated with Rab9 siRNA1 and analyzed by confocal microscopy 48 h after siRNA transfection. (C) AAV2-Luc transduction of HeLa cells treated with Rab9 siRNAs. Cells were infected at various MOIs (10,000, 1,000, or 100 vg/cell) 48 h after siRNA transfection. (D) AAV-Luc transduction (MOI = 10,000) of HEK293T cells transfected with a dominant negative Rab9 plasmid (Rab9-DN). Luciferase values are normalized to the values for cells transfected with a control EGFP plasmid. (E) Validation of Rab7 knockdown by three siRNAs against Rab7 (siRab7-1 to siRab7-3) at 48 h posttransfection. (F) Steady-state localization of Ci-MPR in HeLa cells treated with Rab7 siRNA1 and analyzed by confocal microscopy 48 h after siRNA transfection. (G) AAV2-Luc transduction of HeLa cells treated with Rab7 siRNAs. Cells were infected at various MOIs (10,000, 1,000, or 100 vg/cell) 48 h after siRNA transfection. (H) AAV2-Luc transduction (MOI = 10,000) of HEK293T cells transfected with a dominant negative Rab7 plasmid. Luciferase values are normalized to the values for cells transfected with a control EGFP plasmid. *, $P < 0.05$.

duction), whereas STX6 siRNA had no effect, and STX16 siRNA induced a modest 1.6-fold increase (data not shown). Overall, these results indicate that AAV2 and AAV1 traffic via a noncanonical retrograde pathway that is controlled by STX5.

**Inhibition of AAV transport by compounds affecting STX5.** High-throughput screens for small-molecule inhibitors of ricin toxicity have recently identified Retro-2 to be a specific blocker of retrograde transport acting at the endosome-TGN interface (59),

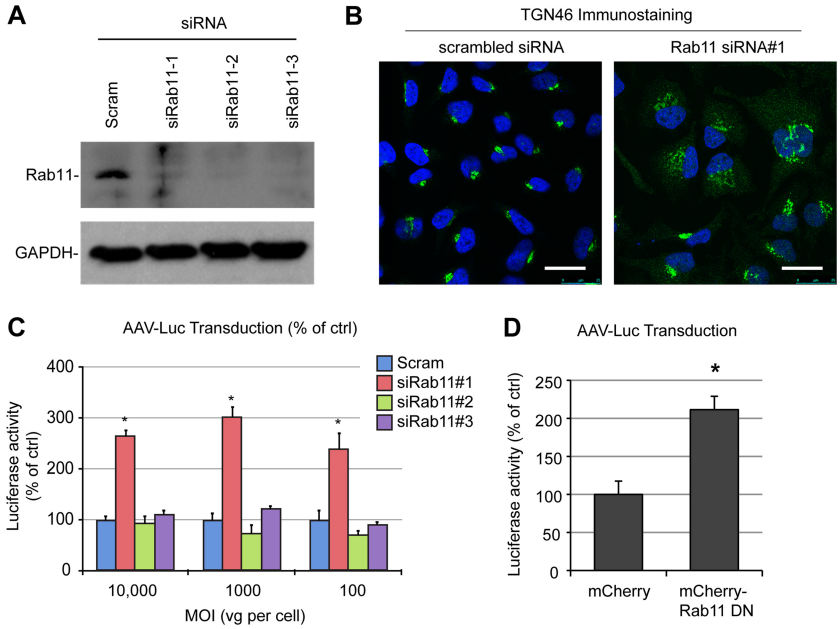


**FIG 5** AAV transduction is independent of recycling endosomes. (A) Validation of siRNA-mediated knockdown of Rab11 by multiple siRNAs (siRab11-1 to siRab11-3). Protein extracts were prepared 48 h after transfection of HeLa cells and analyzed by immunoblotting with an anti-Rab11 antibody. (B) Perturbation of TGN46 retrograde transport in HeLa cells transfected with Rab11 siRNA. Cells were fixed at 48 h posttransfection, stained with an anti-TGN46 antibody, and analyzed by confocal microscopy. (C) AAV2-Luc transduction of HeLa cells treated with Rab11 siRNAs. Cells were infected at various MOIs (10,000, 1,000, or 100 vg/cell) 48 h after siRNA transfection. Luciferase reads are normalized to the amount of control siRNA for each MOI. (D) AAV2-Luc transduction of HEK293T cells transfected with a dominant negative Rab11 plasmid. Values represent the mean and SD from triplicate experiments. *, $P < 0.05$.

and it has been shown that Retro-2 and more potent derivatives (41, 42) block retrograde transport of ricin and Shiga toxin by displacing STX5 from the TGN toward small peripheral vesicles (42, 59). In agreement with our STX5 siRNA data, treatment of HeLa cells with the cyclized analog Retro-$2_{cycl}$ significantly decreased AAV2-Luc transduction in a dose-dependent manner, showing a reduction of approximately 80% at the highest soluble concentration of 100 μM (Fig. 7A). In our hands, the original Retro-2 compound and Retro-$2_{cycl}$ (60) had indistinguishable properties. Because Retro-2 can spontaneously cyclize to Retro-$2_{cycl,}$ both are referred to as Retro-2 in this article. A novel, highly potent derivative of Retro-2, Retro-2.1 (42), showed an ~100-fold improvement of the 50% effective concentration against AAV2 transduction and achieved more than 90% inhibition of transduction at a concentration of 20 μM, the maximal dose tested (Fig. 7A). Importantly, this effect was not attributable to a general cytotoxic effect, since neither compound showed a significant reduction of cell viability after 24 h when tested at the maximal concentration (Fig. 7B). Retro-2.1 showed similar inhibitory effects on AAV2 transduction at low, moderate, and high MOIs (Fig. 7C), suggesting that STX5 is required for AAV2 transduction regardless of the viral dose. Retro-2 and Retro-2.1 also did not interfere with AAV2 endocytosis (Fig. 7D), indicating that inhibition of STX5 function modulates AAV2 transduction at a postentry level. To rule out any possible indirect effect of Retro-2 or Retro-2.1 on reporter gene expression *per se*, we used adenovirus serotype 5-EGFP as a control. Clade C adenoviruses escape directly from early endosomes or macropinosomes into the cytoplasm and do not rely on retrograde transport for infection (61, 62). Neither Retro-2 nor Retro-2.1 had a measurable effect on Ad5-EGFP transduction, even at the highest concentrations tested. These results rule out an artifactual inhibitory effect resulting from cytotoxicity or interference with reporter gene expression (Fig. 7E). Comparative kinetic analysis showed that Retro-2.1 acts at an intermediate step between bafilomycin A1 and golgicide (Fig. 7F), suggesting that STX5 regulates a trafficking mechanism downstream of endosomal acidification and upstream of potential intra-Golgi apparatus transport, consistent with endosome-to-TGN transport. Confocal microscopy analysis of HeLa cells at 3 h postinfection showed that Retro-2.1 induced a moderate dispersal of the TGN, as evidenced by staining with golgin-97, and blocked AAV2 transport to the dispersed TGN, sequestering AAV2 capsids in scattered peripheral vesicles (Fig. 8A). Quantification of the AAV/TGN-colocalized pixels showed a 5-fold reduction of AAV2 translocation to the TGN following Retro-2.1 treatment, a value remarkably similar to the 80 to 90% decrease of transduction resulting from the same drug treatment (see above). As shown in previous studies (42, 59), Retro-2.1 induced a dramatic dispersal of STX5 from the TGN into small peripheral vesicles (Fig. 8C). Most interestingly, in Retro-2.1-treated cells, AAV2 virions accumulated in dispersed STX5-positive vesicles (Fig. 8C), and the colocalization index of AAV2 with STX5 was not affected (Fig. 8D). These observations suggest that Retro-2 disrupts AAV2 trafficking at the endosome/TGN interface, as has been shown previously for ricin and Shiga toxin (59). This is consistent with a model in which the SNARE protein STX5 mediates the fusion of AAV2-containing vesicles with the TGN.

**Conservation of the retrograde transport mechanism of AAV serotypes among various cell types.** Recent data suggest that various AAV serotypes can undergo distinct trafficking pathways, which may, in part, account for variations in transduction efficiency (63). In addition, recent evidence suggests that intracellular processing of AAV shows significant differences between transformed and primary cells (16). Our data suggest that AAV sero-

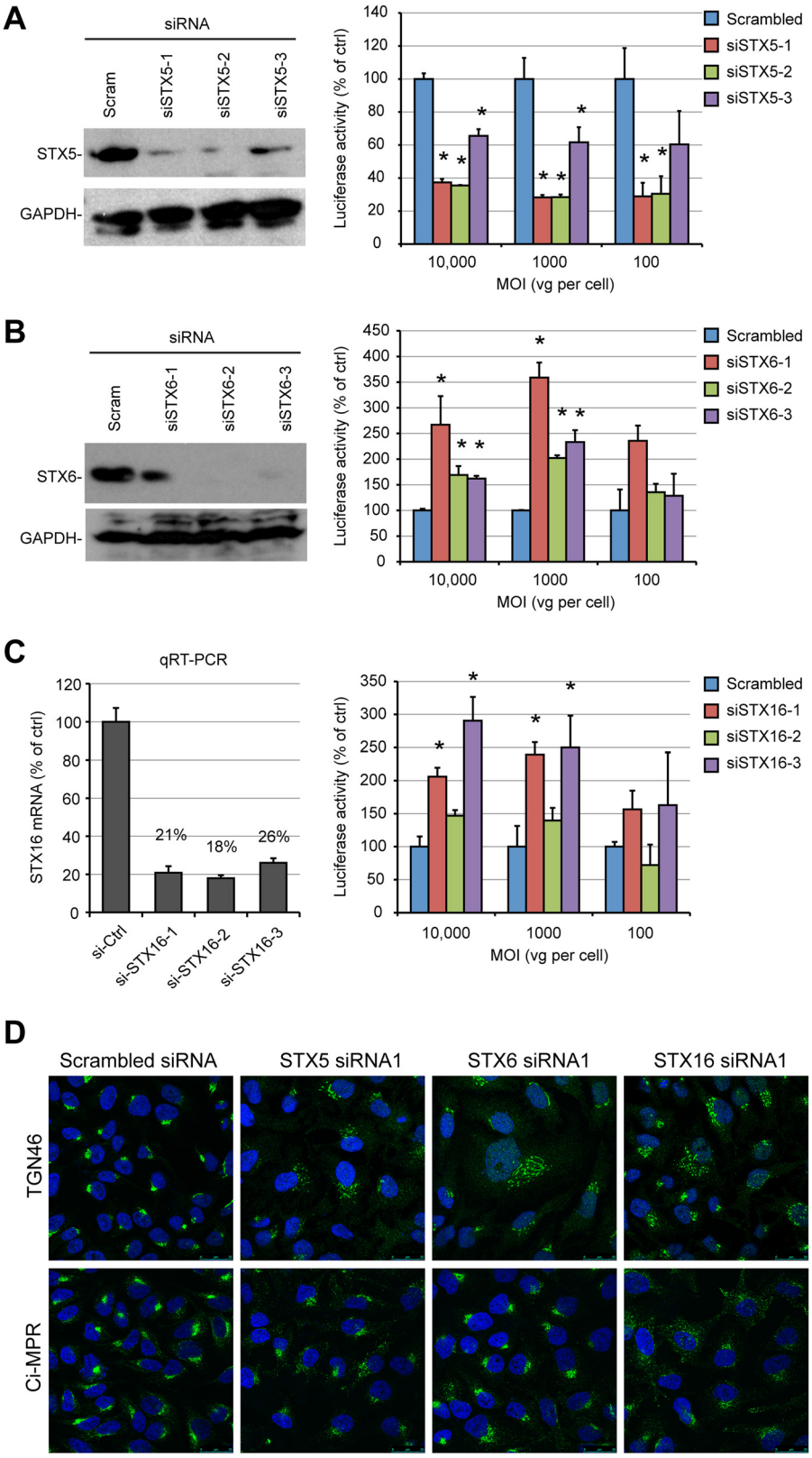


**FIG 6** AAV transduction requires STX5, but not STX6 or STX16. (A) STX5 expression and AAV2-Luc transduction in HeLa cells treated with STX5 siRNAs (siSTX5-1 to siSTX5-3). Protein expression and viral transduction were performed 48 h after siRNA transfection. (B) STX6 expression and AAV2-Luc transduction in HeLa cells treated with STX6 siRNAs (siSTX6-1 to siSTX6-3). (C) STX16 expression and AAV2-Luc transduction in HeLa cells treated with STX16 siRNAs (siSTX16-1 to siSTX16-3). Luciferase activity values on the *y* axes of panels A to C are normalized to those for cells treated with scrambled siRNA and represent the mean ± SD from triplicate experiments. *, $P < 0.05$. (D) Steady-state localization of TGN46 and Ci-MPR in HeLa cells transfected with siRNA against Golgi apparatus-resident STXs. Cells were fixed at 48 h posttransfection and analyzed by confocal microscopy.

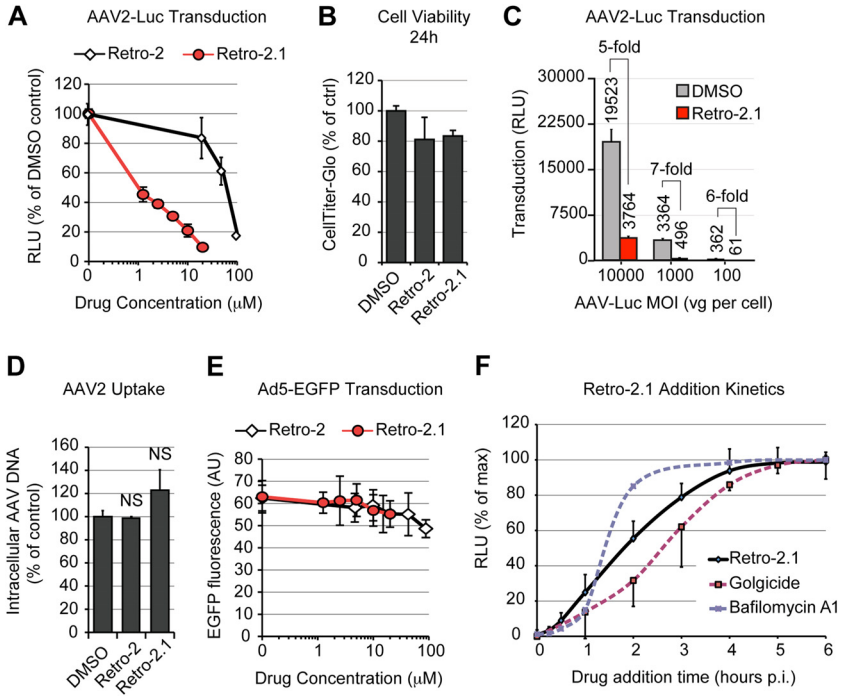


**FIG 7** Inhibitors of STX5 decrease AAV2 transduction and retrograde transport. (A) AAV2-Luc transduction of HeLa cells treated with various concentrations of Retro-2 or Retro-2.1. Cells were pretreated for 30 min at 37°C before addition of AAV2-Luc at an MOI of 10,000 vg/cell. Luciferase activity values are normalized to those for the dimethyl sulfoxide-treated control. (B) Retro-2 and Retro-2.1 are not cytotoxic. HeLa cells were treated with the maximal tested concentrations of Retro-2 (100 μM) and Retro-2.1 (20 μM) for 24 h, and cell viability was measured using the luciferase-based CellTiter-Glo method. (C) AAV2-Luc transduction of HeLa cells at various MOIs in the presence of 10 μM Retro-2.1. Absolute luciferase output and inhibition ratios are indicated. (D) Endocytosis of AAV2-Luc is not reduced in HeLa cells treated with 100 μM Retro-2 or 20 μM Retro-2.1. Intracellular viral DNA was quantified by real-time PCR, and values are normalized to those for the dimethyl sulfoxide-treated control. NS, not significant. (E) Transduction of HeLa cells by Ad5-EGFP in the presence of Retro-2 or Retro-2.1. Values indicate the average ± SD of the green fluorescence intensity per microscope field, expressed in arbitrary units (AU). (F) Kinetics of Retro-2.1 addition. HeLa cells were incubated for 1 h on ice with AAV2-Luc, washed, and transferred to 37°C to trigger infection. Drug was added at various time points, and luciferase activity was measured after 24 h. Dotted lines, the kinetics of golgicide and bafilomycin A1 addition presented in Fig. 1H. Luciferase activity values were normalized to the maximum (plateau) values, as described in the legend of Fig. 1. The values in all panels represent mean and SD from triplicate experiments.

types 1 and 2 use a similar retrograde transport mechanism in HeLa cells (our unpublished observations). Next, we decided to determine if the same pathway is shared by other common AAV serotypes, namely, serotypes 3, 4, 5, 6, 8, and 9, which differ in their tropism and receptor usage (reviewed in reference 2). All tested serotypes showed a significantly decreased transduction in HeLa cells treated by STX5 siRNA (Fig. 9A) or with 100 μM Retro-2 (Fig. 9B). This demonstrates that, in HeLa cells, all tested AAV serotypes require STX5-dependent retrograde transport for transduction, regardless of their primary receptor. Hepatic and cardiovascular tissues are among the most promising targets in AAV-based clinical trials, so we sought to extend our investigations to liver-derived cells and cells from the cardiovascular system. As expected, transduction among the AAV serotypes and cell types varied widely (Fig. 9C to F). Nevertheless, Retro-2 treatment significantly decreased the transduction efficiency of all tested AAVs in the hepatocarcinoma cell lines Huh7 (Fig. 9C) and HepG2 (data not shown), as well as in human umbilical vein endothelial cells (HUVECs), human coronary artery endothelial cells (HCAECs), and adult rat cardiomyocytes (RACMs) (Fig. 9D to F, respectively). The only exception was in cardiomyocytes infected with AAV9, for which no significant difference could be observed (Fig. 9F). It is worth mentioning that primary cardiomyocytes had to be cultured for at least 48 h after infection to reach a level of luciferase activity above the background level. Retro-2 has a half-life of ~24 h in organic solvents (60). Therefore, we cannot exclude the possibility that the drug activity dropped below active levels during the incubation. Consistently, for all serotypes tested, the degree of inhibition observed in RACMs treated with Retro-2 was lower than that observed in the other cell types (Fig. 9F).

Taken together, our data show that AAV transduction relies on a noncanonical, STX5-dependent retrograde transport mechanism toward the TGN and that this distinct pathway is highly conserved among AAV serotypes and cell types.

## DISCUSSION

The intracellular process of AAV trafficking that precedes nuclear import has been studied for years, but it is still incompletely understood. Nevertheless, a number of controversies notwithstanding, a consensus regarding AAV trafficking is slowly emerging. Following receptor binding, AAV is endocytosed into early endosomal vesicles. Acidification of these carriers triggers a conformational change in the AAV capsid and exposes the N-terminal domain of the minor capsid protein VP1 on the capsid surface (13). $VP1_u$ contains a phospholipase A2 (PLA2) domain that mediates the egress of AAV capsids into the cytoplasm (11, 64, 65). From the cytoplasm, intact capsids are then translocated across the nuclear envelope to deliver their DNA payload to the nucleus

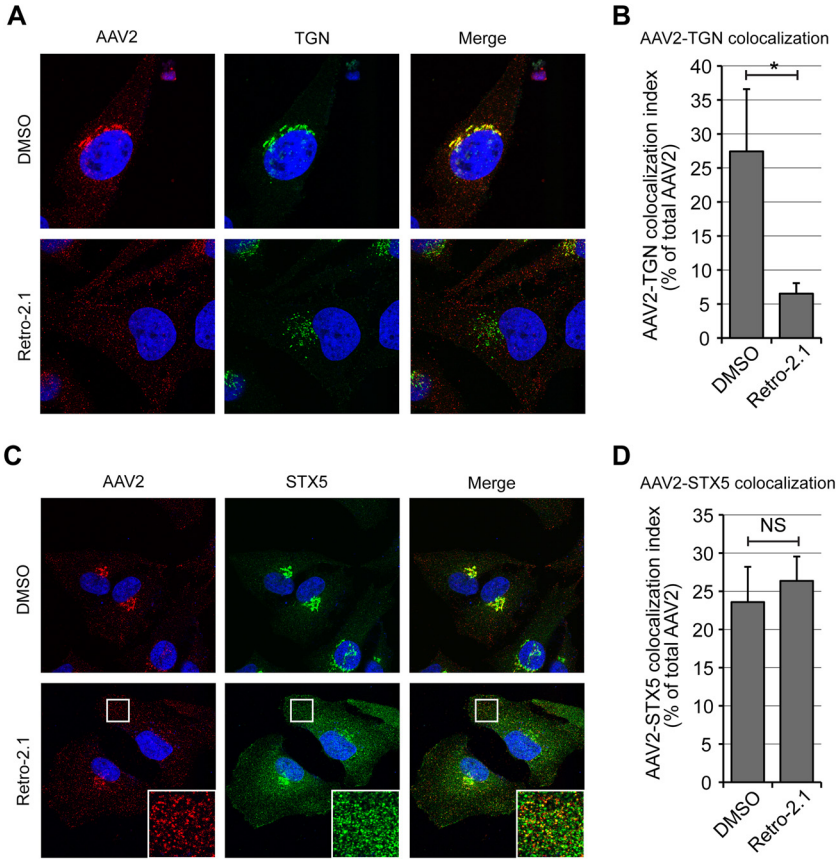


**FIG 8** Retro-2.1 blocks endosome-to-TGN transport of AAV2. (A) HeLa cells were infected with AAV2-Luc at an MOI of 10,000 vg/cell in the presence of 20 μM Retro-2.1 or dimethyl sulfoxide. Cells were fixed at 3 h after infection and stained for AAV2 capsids (red) and golgin-97 (green) before imaging by confocal microscopy. (B) Quantification of the colocalization index between AAV2 capsids and golgin-97. Values represent the percentage of red pixels overlapping with green pixels. *, $P < 0.05$. (C) HeLa cells were treated as described in the legend to panel A and stained for AAV2 capsids (red) and STX5 (green). (Insets) Higher magnifications of boxed areas. (D) Quantification of the colocalization index between AAV2 capsids and STX5. Values represent the percentage of red pixels overlapping with green pixels. NS, not significant.

(13–15). The identity of the subcellular compartment from which AAV escapes into the cytoplasm has not been established but may be of great importance for rational vector design because escape from the endosomal system might be a rate-limiting step in AAV transduction. Others and we reported that a significant portion of AAV capsids traffic to the TGN and the Golgi apparatus (5, 23–25), but the significance of this trafficking pathway in AAV transduction has not been firmly established. Our present experiments show that drugs that target Golgi apparatus trafficking, such as brefeldin A and the more specific compounds golgicide A and Retro-2, all inhibit AAV2 transduction, and our data obtained with poorly permissive cells are consistent with a model in which the efficacy of transport to the Golgi apparatus correlates with the natural susceptibility to AAV2 infection (Fig. 1 and our unpublished data). Together, our results strongly suggest that retrograde transport of AAV to the TGN/Golgi complex is an absolute requirement for gene delivery. Interestingly, bafilomycin A1 treatment blocked AAV transduction but did not prevent AAV trafficking to the Golgi apparatus (Fig. 1). This suggests that the exposure of the VP1 PLA2 domain in acidic endosomes is a prerequisite for transduction regardless of Golgi apparatus trafficking. But why then is transport to the TGN/Golgi apparatus required for transduction? The simplest model is based on the hypothesis that the conditions for extrusion of $VP1_u$ and conditions at which the $VP1_u$ PLA2 domain is enzymatically active are spatiotemporally distinct and mutually exclusive. Consistent with this hypothesis, the process of endosomal acidification, which is absolutely necessary for $VP1_u$ PLA2 domain exposure and AAV transduction, requires active export of calcium ions from the endosomal lumen (66). As a result, acidic endosomes contain only minute concentrations (~3 μM) of $Ca^{2+}$ (66). At these $Ca^{2+}$ concentrations, the phospholipase A2 of AAV is inactive (67–69). Because AAV transduction is dependent on $VP1_u$ PLA2 activity, this means that AAV must be transported to a postendocytic, calcium-rich subcellular compartment such as the TGN/Golgi apparatus ($[Ca^{2+}]$, ~300 μM) or the ER ($[Ca^{2+}]$, ~400 μM) (70) for optimal activity (67–69). Put differently, according to this model, AAV capsids are exposed to acidic pH shortly after endocytosis, triggering $VP1_u$ extrusion, and are then transported along a STX5-dependent retrograde route to the calcium-rich TGN/Golgi apparatus. The nearly optimal $Ca^{2+}$ concentration in the TGN/Golgi apparatus would then trigger the activation of the surface-exposed PLA2, leading to escape into the cytoplasm (Fig. 10). The temporal order of such a stepwise process is indeed consistent with our differential kinetics results (Fig. 1 and 7). Unlike most extracellular retrograde transport cargos described so far (71), we did not

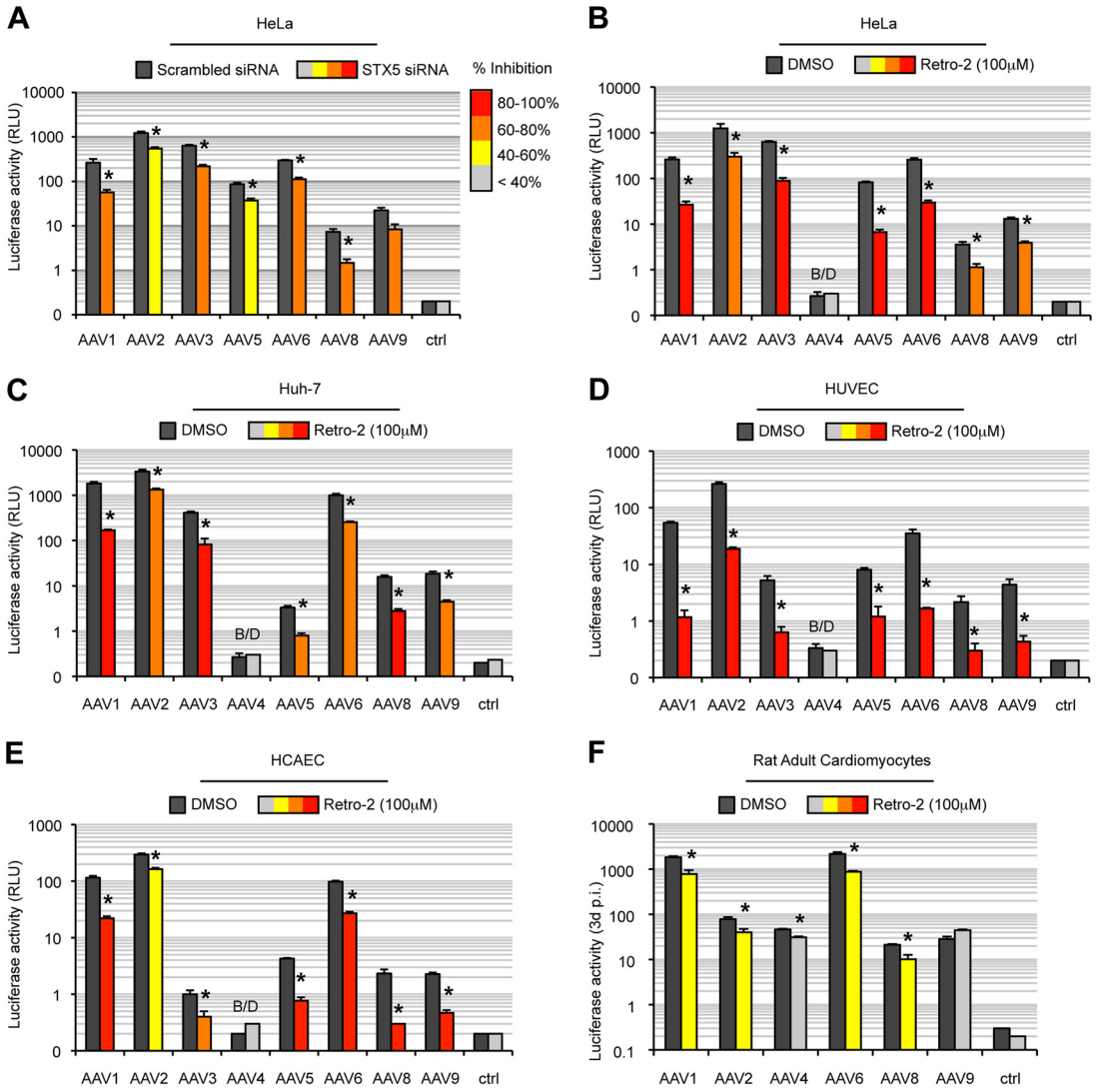


**FIG 9** STX5-dependent transport is conserved among AAV serotypes and cell types. (A) Transduction of HeLa cells by different AAV serotypes containing a luciferase expression cassette, performed 48 h after STX5 siRNA transfection. Values indicate the luciferase activity normalized to the activity for scrambled siRNA-treated cells. (B to F) AAV serotypes 1, 2, 3, 4, 5, 6, 8, and 9 containing a luciferase expression cassette (MOI = 10,000 vg/cell) were used to infect HeLa cells (B), Huh7 cells (C), HUVECs (D), HCAECs (E), or RACMs (F) pretreated with 100 μM Retro-2. Luciferase values are normalized to those for dimethyl sulfoxide-treated cells. All values represent the mean ± SD from triplicate experiments. *, $P < 0.05$ by two-tailed Student's *t* test. B/D, below the detection limit.

find evidence for Golgi apparatus-to-ER transport of AAV capsids. The simplest explanation for this observation is that virions escape the endosomal system directly from the TGN/Golgi compartment. However, on the basis of our present data, we cannot rule out the possibility that transport of AAV to the ER is rate limiting and that AAV rapidly escapes into the cytoplasm once it reaches the ER. Further studies will be needed to address this point.

To define further the endosome-to-TGN route of AAV capsids, we targeted specific cellular factors that are known to be crucial for classical retrograde transport pathways. Surprisingly, and in contrast to findings published in the literature (19), AAV transduction was not affected by the disruption of the two major retrograde pathways, the EE-RE-TGN or the EE-LE-TGN route, regardless of the multiplicity of infection used. In particular, our findings obtained using multiple siRNAs to silence Rab7, Rab9, and Rab11 expression, together with our findings obtained using dominant negative mutants of Rab7, Rab9, and Rab11 (Fig. 4 and 5), rule out the involvement of late or recycling endosomes in AAV2 transduction. This was unexpected because previous studies suggested that, depending on the MOI used, AAV2 trafficking was dependent on either late or recycling endosomes (19). We do not have an explanation for this discrepancy, but we observed that individual siRNA sequences could exert artifactual effects on AAV transduction. As the study from Ding and colleagues (19) relied on a single siRNA against Rab7 or Rab11 to disrupt late or recycling endosomes, respectively, it is possible that some of their observations resulted from off-target effects. Of note, our observations do not conflict with published results that Rab7-positive late endosomes are used for long-distance, retrograde axonal transport of AAV toward the cell body in neurons (21). We have previously shown that AAV2 transduction, at least in HeLa and HEK293T cells, is largely unaf-

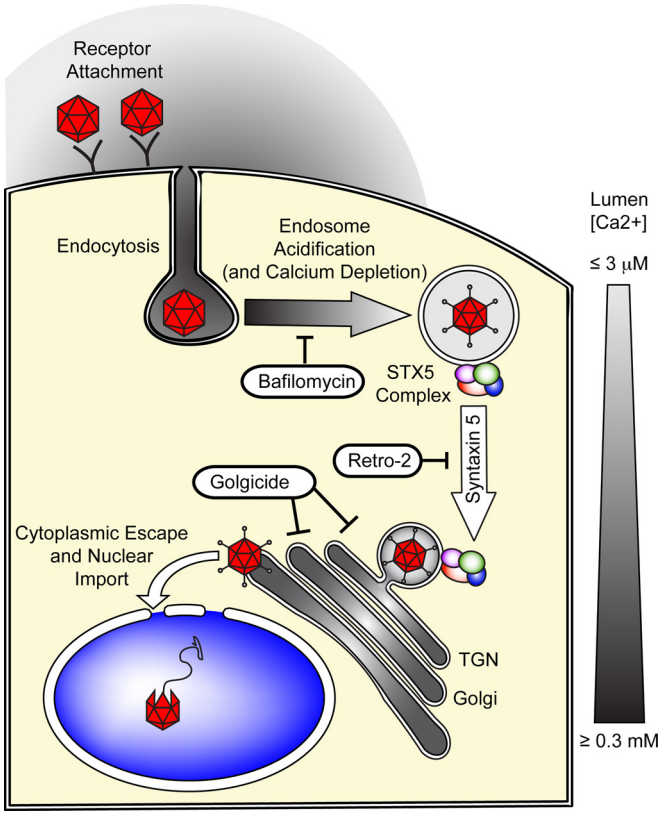


**FIG 10** Hypothetical model of syntaxin 5-dependent transport of AAV to the TGN/Golgi apparatus. Following receptor attachment and endocytosis, early endocytic vesicles are rapidly acidified, which can be inhibited by the proton ATPase inhibitor bafilomycin A1. This endosomal acidification is dependent on the depletion of endosomal calcium. The acidic environment of the endosomes and, presumably, the proteolytic cleavage of AAV capsid proteins trigger the extrusion of the unique, PLA2-containing region of the largest capsid protein, VP1. However, as a result of the minute calcium concentrations in the endosomes, the PLA2 is enzymatically inactive. AAV is then transported to the TGN/Golgi apparatus, and this transport can be inhibited with the GBF1 inhibitor golgicide. This endosome-to-TGN/Golgi apparatus transport step is also dependent on the tSNARE STX5, whose function can be inhibited by Retro-2 and its derivatives or by siRNA-mediated knockdown of STX5. The calcium concentration in the TGN/Golgi apparatus, which is near the optimal level for VP1-PLA2 activity, then allows escape into the cytoplasm, followed by nuclear import and uncoating of the AAV capsid.

fected by dynamin inhibition (5), which further rules out the dynamin-dependent EE-TGN pathway used by Shiga toxin, ricin, and Ci-MPR (5, 72). In light of the present findings, it is tempting to speculate that the nonclassical clathrin-independent carrier (CLIC) endosomes involved in productive AAV2 internalization (5) target the virions toward a distinct, atypical pathway to the TGN, which was previously suggested to be used by glycosylphosphatidylinositol-anchored proteins (73).

Whereas the precise nature of this noncanonical route needs to be elucidated fully, our data clearly show that the retrograde transport of AAV is controlled by STX5, since both STX5 siRNA and Retro-2 significantly reduced AAV transduction efficiency (Fig. 6 to 9). Our kinetics experiments also indicate that STX5 acts at an intermediate level between endosomal acidification and the transport to the Golgi apparatus, which is consistent with a role of STX5 in the endosome-to-TGN transport step, as previously described for ricin and Shiga toxin (59). In cells treated with the highly potent analog Retro-2.1, STX5 was rapidly displaced from the TGN to a large number of small peripheral vesicles, and AAV2 capsid transport to the TGN was severely impaired. Strikingly, the colocalization of AAV2 capsids and STX5 was not affected by Retro-2.1 treatment. This suggests that the tSNARE STX5 is critical for the fusion of a subset of endocytic vesicles with the TGN and that Retro-2.1 blocks this process by interfering with STX5 shuttling. As a result, AAV2 capsids are sequestered in peripheral STX5-positive vesicles. Interestingly, in most cell types studied, other common AAV serotypes were also sensitive to inhibition of STX5 function, irrespective of their primary binding receptors (Fig. 9). The sole exception was transduction of adult rat cardiomyocytes by AAV9, which is in line with the unique properties of AAV9 and adult cardiomyocytes (37, 74, 75).

The sorting of endocytic cargos into a particular route is generally determined by specific motifs on the cytoplasmic tail of transmembrane receptors (76), and a recent study suggests that distinct AAV serotypes may differ in their endocytosis rates and trafficking mechanisms (7, 63). Therefore, the finding that various serotypes appear to converge into a single retrograde transport pathway was unexpected. However, we found that in HeLa cells, transduction by all common AAV serotypes was strongly inhibited by GRAF1 siRNA (our unpublished data), and GRAF1 is the most definitive marker of CLIC/GEEC endocytosis (77). This would suggest that the CLIC/GEEC pathway represents a general endocytic mechanism for effective AAV infection, at least in HeLa cells. If CLIC/GEEC endocytosis were the most efficient endocytic route for all common AAV serotypes, it would not be unexpected that all AAV capsids would converge into a common retrograde transport route leading to the TGN.

In summary, our data demonstrate that AAV follows a noncanonical, STX5-dependent pathway to the TGN/Golgi apparatus that is indispensable for transduction. Further dissection of this trafficking route will undoubtedly yield critical insights into AAV biology and promises to facilitate the development of AAV vectors with improved properties.

## ACKNOWLEDGMENTS

We thank Kirsten Sadler Edepli and Chuan Gao (Icahn School of Medicine at Mount Sinai, New York, NY) for the ER-tdTmt plasmid. We are grateful to Ludger Johannes (Institut Curie, Paris, France) for helpful discussion and advice. We gratefully acknowledge the continuous support by Roger J. Hajjar (Icahn School of Medicine at Mount Sinai, New York, NY).

This work was supported by U.S. National Institutes of Health grants R01 HL117505 (to Roger J. Hajjar) and R01 HL 119046 (to Roger J. Hajjar). M.E.N. was supported by NIH training grants T32DK007757 and T32HL007824. J.-C.C. and D.G. were funded by the French National Agency for Research (ANR) under contract ANR-11-BSV2-0018, the Joint Ministerial Program of R&D against CBRNe Risks, and CEA.

## REFERENCES

1. **Grimm D, Kay MA.** 2003. From virus evolution to vector revolution: use of naturally occurring serotypes of adeno-associated virus (AAV) as novel vectors for human gene therapy. Curr Gene Ther **3:**281–304. http://dx.doi.org/10.2174/1566523034578285.
2. **Nonnenmacher M, Weber T.** 2012. Intracellular transport of recombinant adeno-associated virus vectors. Gene Ther **19:**649–658. http://dx.doi.org/10.1038/gt.2012.6.
3. **Bartlett JS, Wilcher R, Samulski RJ.** 2000. Infectious entry pathway of adeno-associated virus and adeno-associated virus vectors. J Virol **74:**2777–2785. http://dx.doi.org/10.1128/JVI.74.6.2777-2785.2000.
4. **Duan D, Li Q, Kao AW, Yue Y, Pessin JE, Engelhardt JF.** 1999.

Dynamin is required for recombinant adeno-associated virus type 2 infection. J Virol **73:**10371–10376.
5. **Nonnenmacher M, Weber T.** 2011. Adeno-associated virus 2 infection requires endocytosis through the CLIC/GEEC pathway. Cell Host Microbe **10:**563–576. http://dx.doi.org/10.1016/j.chom.2011.10.014.
6. **Uhrig S, Coutelle O, Wiehe T, Perabo L, Hallek M, Buning H.** 2012. Successful target cell transduction of capsid-engineered rAAV vectors requires clathrin-dependent endocytosis. Gene Ther **19:**210–218. http://dx.doi.org/10.1038/gt.2011.78.
7. **Weinberg MS, Nicolson S, Bhatt AP, McLendon M, Li C, Samulski RJ.** 2014. Recombinant adeno-associated virus utilizes cell-specific infectious entry mechanisms. J Virol **88:**12472–12484. http://dx.doi.org/10.1128/JVI.01971-14.
8. **Douar AM, Poulard K, Stockholm D, Danos O.** 2001. Intracellular trafficking of adeno-associated virus vectors: routing to the late endosomal compartment and proteasome degradation. J Virol **75:**1824–1833. http://dx.doi.org/10.1128/JVI.75.4.1824-1833.2001.
9. **Akache B, Grimm D, Shen X, Fuess S, Yant SR, Glazer DS, Park J, Kay MA.** 2007. A two-hybrid screen identifies cathepsins B and L as uncoating factors for adeno-associated virus 2 and 8. Mol Ther **15:**330–339. http://dx.doi.org/10.1038/sj.mt.6300053.
10. **Kronenberg S, Bottcher B, von der Lieth CW, Bleker S, Kleinschmidt JA.** 2005. A conformational change in the adeno-associated virus type 2 capsid leads to the exposure of hidden VP1 N termini. J Virol **79:**5296–5303. http://dx.doi.org/10.1128/JVI.79.9.5296-5303.2005.
11. **Stahnke S, Lux K, Uhrig S, Kreppel F, Hösel M, Coutelle O, Ogris M, Hallek M, Büning H.** 2011. Intrinsic phospholipase A2 activity of adeno-associated virus is involved in endosomal escape of incoming particles. Virology **409:**77–83. http://dx.doi.org/10.1016/j.virol.2010.09.025.
12. **Girod A, Wobus CE, Zadori Z, Ried M, Leike K, Tijssen P, Kleinschmidt JA, Hallek M.** 2002. The VP1 capsid protein of adeno-associated virus type 2 is carrying a phospholipase A2 domain required for virus infectivity. J Gen Virol **83:**973–978.
13. **Sonntag F, Bleker S, Leuchs B, Fischer R, Kleinschmidt JA.** 2006. Adeno-associated virus type 2 capsids with externalized VP1/VP2 trafficking domains are generated prior to passage through the cytoplasm and are maintained until uncoating occurs in the nucleus. J Virol **80:**11040–11054. http://dx.doi.org/10.1128/JVI.01056-06.
14. **Grieger JC, Snowdy S, Samulski RJ.** 2006. Separate basic region motifs within the adeno-associated virus capsid proteins are essential for infectivity and assembly. J Virol **80:**5199–5210. http://dx.doi.org/10.1128/JVI.02723-05.
15. **Nicolson SC, Samulski RJ.** 2014. Recombinant adeno-associated virus utilizes host cell nuclear import machinery to enter the nucleus. J Virol **88:**4132–4144. http://dx.doi.org/10.1128/JVI.02660-13.
16. **Johnson J, Li C, Diprimio N, Weinberg M, McCown T, Samulski R.** 2010. Mutagenesis of adeno-associated virus type 2 capsid protein VP1 uncovers new roles for basic amino acids in trafficking and cell-specific transduction. J Virol **84:**8888–8902. http://dx.doi.org/10.1128/JVI.00687-10.
17. **Ding W, Yan Z, Zak R, Saavedra M, Rodman DM, Engelhardt JF.** 2003. Second-strand genome conversion of adeno-associated virus type 2 (AAV-2) and AAV-5 is not rate limiting following apical infection of polarized human airway epithelia. J Virol **77:**7361–7366. http://dx.doi.org/10.1128/JVI.77.13.7361-7366.2003.
18. **Hauck B, Zhao W, High K, Xiao W.** 2004. Intracellular viral processing, not single-stranded DNA accumulation, is crucial for recombinant adeno-associated virus transduction. J Virol **78:**13678–13686. http://dx.doi.org/10.1128/JVI.78.24.13678-13686.2004.
19. **Ding W, Zhang LN, Yeaman C, Engelhardt JF.** 2006. rAAV2 traffics through both the late and the recycling endosomes in a dose-dependent fashion. Mol Ther **13:**671–682. http://dx.doi.org/10.1016/j.ymthe.2005.12.002.
20. **Xiao W, Warrington KH, Jr, Hearing P, Hughes J, Muzyczka N.** 2002. Adenovirus-facilitated nuclear translocation of adeno-associated virus type 2. J Virol **76:**11505–11517. http://dx.doi.org/10.1128/JVI.76.22.11505-11517.2002.
21. **Castle MJ, Perlson E, Holzbaur ELF, Wolfe JH.** 2014. Long-distance axonal transport of AAV9 is driven by dynein and kinesin-2 and is trafficked in a highly motile Rab7-positive compartment. Mol Ther **22:**554–566. http://dx.doi.org/10.1038/mt.2013.237.
22. **Xiao PJ, Samulski RJ.** 2012. Cytoplasmic trafficking, endosomal escape, and perinuclear accumulation of adeno-associated virus type 2 particles are facilitated by microtubule network. J Virol **86:**10462–10473. http://dx.doi.org/10.1128/JVI.00935-12.
23. **Pajusola K, Gruchala M, Joch H, Luscher TF, Yla-Herttuala S, Bueler H.** 2002. Cell-type-specific characteristics modulate the transduction efficiency of adeno-associated virus type 2 and restrain infection of endothelial cells. J Virol **76:**11530–11540. http://dx.doi.org/10.1128/JVI.76.22.11530-11540.2002.
24. **Bantel-Schaal U, Hub B, Kartenbeck J.** 2002. Endocytosis of adeno-associated virus type 5 leads to accumulation of virus particles in the Golgi compartment. J Virol **76:**2340–2349. http://dx.doi.org/10.1128/jvi.76.5.2340-2349.2002.
25. **Johnson JS, Gentzsch M, Zhang LQ, Ribeiro CMP, Kantor B, Kafri T, Pickles RJ, Samulski RJ.** 2011. AAV exploits subcellular stress associated with inflammation, endoplasmic reticulum expansion, and misfolded proteins in models of cystic fibrosis. PLoS Pathog **7:**e1002053. http://dx.doi.org/10.1371/journal.ppat.1002053.
26. **Johannes L, Popoff V.** 2008. Tracing the retrograde route in protein trafficking. Cell **135:**1175–1187. http://dx.doi.org/10.1016/j.cell.2008.12.009.
27. **Sandvig K, Grimmer S, Lauvrak SU, Torgersen ML, Skretting G, van Deurs B, Iversen TG.** 2002. Pathways followed by ricin and Shiga toxin into cells. Histochem Cell Biol **117:**131–141. http://dx.doi.org/10.1007/s00418-001-0346-2.
28. **Sandvig K, van Deurs B.** 2005. Delivery into cells: lessons learned from plant and bacterial toxins. Gene Ther **12:**865–872. http://dx.doi.org/10.1038/sj.gt.3302525.
29. **Day PM, Thompson CD, Schowalter RM, Lowy DR, Schiller JT.** 2013. Identification of a role for the *trans*-Golgi network in human papillomavirus 16 pseudovirus infection. J Virol **87:**3862–3870. http://dx.doi.org/10.1128/JVI.03222-12.
30. **Lipovsky A, Popa A, Pimienta G, Wyler M, Bhan A, Kuruvilla L, Guie MA, Poffenberger AC, Nelson CDS, Atwood WJ, DiMaio D.** 2013. Genome-wide siRNA screen identifies the retromer as a cellular entry factor for human papillomavirus. Proc Natl Acad Sci U S A **110:**7452–7457. http://dx.doi.org/10.1073/pnas.1302164110.
31. **Lombardi D, Soldati T, Riederer MA, Goda Y, Zerial M, Pfeffer SR.** 1993. Rab9 functions in transport between late endosomes and the trans Golgi network. EMBO J **12:**677–682.
32. **Chia PZC, Gasnereau I, Lieu ZZ, Gleeson PA.** 2011. Rab9-dependent retrograde transport and endosomal sorting of the endopeptidase furin. J Cell Sci **124:**2401–2413. http://dx.doi.org/10.1242/jcs.083782.
33. **Ganley IG, Espinosa E, Pfeffer SR.** 2008. A syntaxin 10-SNARE complex distinguishes two distinct transport routes from endosomes to the trans-Golgi in human cells. J Cell Biol **180:**159–172. http://dx.doi.org/10.1083/jcb.200707136.
34. **Mallard F, Antony C, Tenza D, Salamero J, Goud B, Johannes L.** 1998. Direct pathway from early/recycling endosomes to the Golgi apparatus revealed through the study of Shiga toxin B-fragment transport. J Cell Biol **143:**973–990. http://dx.doi.org/10.1083/jcb.143.4.973.
35. **Wilcke M, Johannes L, Galli T, Mayau V, Goud B, Salamero J.** 2000. Rab11 regulates the compartmentalization of early endosomes required for efficient transport from early endosomes to the trans-Golgi network. J Cell Biol **151:**1207–1220. http://dx.doi.org/10.1083/jcb.151.6.1207.
36. **Mallard F, Tang BL, Galli T, Tenza D, Saint-Pol A, Yue X, Antony C, Hong W, Goud B, Johannes L.** 2002. Early/recycling endosomes-to-TGN transport involves two SNARE complexes and a Rab6 isoform. J Cell Biol **156:**653–664. http://dx.doi.org/10.1083/jcb.200110081.
37. **Chaanine AH, Nonnenmacher M, Kohlbrenner E, Jin D, Kovacic JC, Akar FG, Najjar RJ, Weber T.** 2014. Effect of bortezomib on the efficacy of AAV9.SERCA2a treatment to preserve cardiac function in a rat pressure-overload model of heart failure. Gene Ther **21:**379–386. http://dx.doi.org/10.1038/gt.2014.7.
38. **Grimm D, Kern A, Rittner K, Kleinschmidt JA.** 1998. Novel tools for production and purification of recombinant adenoassociated virus vectors. Hum Gene Ther **9:**2745–2760. http://dx.doi.org/10.1089/hum.1998.9.18-2745.
39. **Grimm D, Kay MA, Kleinschmidt JA.** 2003. Helper virus-free, optically controllable, and two-plasmid-based production of adeno-associated virus vectors of serotypes 1 to 6. Mol Ther **7:**839–850. http://dx.doi.org/10.1016/S1525-0016(03)00095-9.
40. **Zolotukhin S, Byrne BJ, Mason E, Zolotukhin I, Potter M, Chesnut K, Summerford C, Samulski RJ, Muzyczka N.** 1999. Recombinant adeno-associated virus purification using novel methods improves infectious

titer and yield. Gene Ther **6:**973–985. http://dx.doi.org/10.1038/sj.gt.3300938.
41. **Gupta N, Pons V, Noel R, Buisson DA, Michau A, Johannes L, Gillet D, Barbier J, Cintrat JC.** 2013. (S)-N-Methyldihydroquinazolinones are the active enantiomers of Retro-2 derived compounds against toxins. ACS Med Chem Lett **5:**94–97. http://dx.doi.org/10.1021/ml400457j.
42. **Noel R, Gupta N, Pons V, Goudet A, Garcia-Castillo MD, Michau A, Martinez J, Buisson DA, Johannes L, Gillet D, Barbier J, Cintrat JC.** 2013. N-Methyldihydroquinazolinone derivatives of Retro-2 with enhanced efficacy against Shiga toxin. J Med Chem **56:**3404–3413. http://dx.doi.org/10.1021/jm4002346.
43. **Fujiwara T, Oda K, Yokota S, Takatsuki A, Ikehara Y.** 1988. Brefeldin A causes disassembly of the Golgi complex and accumulation of secretory proteins in the endoplasmic reticulum. J Biol Chem **263:**18545–18552.
44. **Lippincott-Schwartz J, Yuan L, Tipper C, Amherdt M, Orci L, Klausner RD.** 1991. Brefeldin A's effects on endosomes, lysosomes, and the TGN suggest a general mechanism for regulating organelle structure and membrane traffic. Cell **67:**601–616. http://dx.doi.org/10.1016/0092-8674(91)90534-6.
45. **Pelham HRB.** 1991. Multiple targets for brefeldin A. Cell **67:**449–451. http://dx.doi.org/10.1016/0092-8674(91)90517-3.
46. **Saenz JB, Sun WJ, Chang JW, Li JM, Bursulaya B, Gray NS, Haslam DB.** 2009. Golgicide A reveals essential roles for GBF1 in Golgi assembly and function. Nat Chem Biol **5:**157–165. http://dx.doi.org/10.1038/nchembio.144.
47. **Spooner RA, Watson P, Smith DC, Boal F, Amessou M, Johannes L, Clarkson GJ, Lord JM, Stephens DJ, Roberts LM.** 2008. The secretion inhibitor Exo2 perturbs trafficking of Shiga toxin between endosomes and the trans-Golgi network. Biochem J **414:**471–484. http://dx.doi.org/10.1042/BJ20080149.
48. **Hansen J, Qing K, Kwon HJ, Mah C, Srivastava A.** 2000. Impaired intracellular trafficking of adeno-associated virus type 2 vectors limits efficient transduction of murine fibroblasts. J Virol **74:**992–996. http://dx.doi.org/10.1128/JVI.74.2.992-996.2000.
49. **Hansen J, Qing K, Srivastava A.** 2001. Adeno-associated virus type 2-mediated gene transfer: altered endocytic processing enhances transduction efficiency in murine fibroblasts. J Virol **75:**4080–4090. http://dx.doi.org/10.1128/JVI.75.9.4080-4090.2001.
50. **Palokangas H, Ying M, Vaananen K, Saraste J.** 1998. Retrograde transport from the pre-Golgi intermediate compartment and the Golgi complex is affected by the vacuolar $H^+$-ATPase inhibitor bafilomycin A1. Mol Biol Cell **9:**3561–3578. http://dx.doi.org/10.1091/mbc.9.12.3561.
51. **Geiger R, Andritschke D, Friebe S, Herzog F, Luisoni S, Heger T, Helenius A.** 2011. BAP31 and BiP are essential for dislocation of SV40 from the endoplasmic reticulum to the cytosol. Nat Cell Biol **13:**1305–1314. http://dx.doi.org/10.1038/ncb2339.
52. **Sandvig K, van Deurs B.** 2002. Transport of protein toxins into cells: pathways used by ricin, cholera toxin and Shiga toxin. FEBS Lett **529:**49–53. http://dx.doi.org/10.1016/S0014-5793(02)03182-4.
53. **Arighi CN, Hartnell LM, Aguilar RC, Haft CR, Bonifacino JS.** 2004. Role of the mammalian retromer in sorting of the cation-independent mannose 6-phosphate receptor. J Cell Biol **165:**123–133. http://dx.doi.org/10.1083/jcb.200312055.
54. **Bucci C, Thomsen P, Nicoziani P, McCarthy J, van Deurs B.** 2000. Rab7: a key to lysosome biogenesis. Mol Biol Cell **11:**467–480. http://dx.doi.org/10.1091/mbc.11.2.467.
55. **Sollner T, Whiteheart SW, Brunner M, Erdjument-Bromage H, Geromanos S, Tempst P, Rothman JE.** 1993. SNAP receptors implicated in vesicle targeting and fusion. Nature **362:**318–324. http://dx.doi.org/10.1038/362318a0.
56. **McNew JA, Parlati F, Fukuda R, Johnston RJ, Paz K, Paumet F, Sollner TH, Rothman JE.** 2000. Compartmental specificity of cellular membrane fusion encoded in SNARE proteins. Nature **407:**153–159. http://dx.doi.org/10.1038/35025000.
57. **Weber T, Zemelman BV, McNew JA, Westermann B, Gmachl M, Parlati F, Sollner TH, Rothman JE.** 1998. SNAREpins: minimal machinery for membrane fusion. Cell **92:**759–772. http://dx.doi.org/10.1016/S0092-8674(00)81404-X.
58. **Amessou M, Fradagrada A, Falguieres T, Lord JM, Smith DC, Roberts LM, Lamaze C, Johannes L.** 2007. Syntaxin 16 and syntaxin 5 are required for efficient retrograde transport of several exogenous and endogenous cargo proteins. J Cell Sci **120:**1457–1468. http://dx.doi.org/10.1242/jcs.03436.
59. **Stechmann B, Bai SK, Gobbo E, Lopez R, Merer G, Pinchard S, Panigai L, Tenza D, Raposo G, Beaumelle B, Sauvaire D, Gillet D, Johannes L, Barbier J.** 2010. Inhibition of retrograde transport protects mice from lethal ricin challenge. Cell **141:**231–242. http://dx.doi.org/10.1016/j.cell.2010.01.043.
60. **Park JG, Kahn JN, Tumer NE, Pang YP.** 2012. Chemical structure of Retro-2, a compound that protects cells against ribosome-inactivating proteins. Sci Rep **2:**631. http://dx.doi.org/10.1038/srep00631.
61. **Meier O, Boucke K, Hammer SV, Keller S, Stidwill RP, Hemmi S, Greber UF.** 2002. Adenovirus triggers macropinocytosis and endosomal leakage together with its clathrin-mediated uptake. J Cell Biol **158:**1119–1131. http://dx.doi.org/10.1083/jcb.200112067.
62. **Wiethoff CM, Wodrich H, Gerace L, Nemerow GR.** 2005. Adenovirus protein VI mediates membrane disruption following capsid disassembly. J Virol **79:**1992–2000. http://dx.doi.org/10.1128/JVI.79.4.1992-2000.2005.
63. **Keiser NW, Yan ZY, Zhang YL, Lei-Butters DCM, Engelhardt JF.** 2011. Unique characteristics of AAV1, 2, and 5 viral entry, intracellular trafficking, and nuclear import define transduction efficiency in HeLa cells. Hum Gene Ther **22:**1433–1444. http://dx.doi.org/10.1089/hum.2011.044.
64. **Li CW, He Y, Nicolson S, Hirsch M, Weinberg MS, Zhang P, Kafri T, Samulski RJ.** 2013. Adeno-associated virus capsid antigen presentation is dependent on endosomal escape. J Clin Invest **123:**1390–1401. http://dx.doi.org/10.1172/JCI66611.
65. **Farr GA, Zhang LG, Tattersall P.** 2005. Parvoviral virions deploy a capsid-tethered lipolytic enzyme to breach the endosomal membrane during cell entry. Proc Natl Acad Sci U S A **102:**17148–17153. http://dx.doi.org/10.1073/pnas.0508477102.
66. **Gerasimenko JV, Tepikin AV, Petersen OH, Gerasimenko OV.** 1998. Calcium uptake via endocytosis with rapid release from acidifying endosomes. Curr Biol **8:**1335–1338. http://dx.doi.org/10.1016/S0960-9822(07)00565-9.
67. **Dorsch S, Liebisch G, Kaufmann B, von Landenberg P, Hoffmann JH, Drobnik W, Modrow S.** 2002. The VP1 unique region of parvovirus B19 and its constituent phospholipase A2-like activity. J Virol **76:**2014–2018. http://dx.doi.org/10.1128/JVI.76.4.2014-2018.2002.
68. **Zadori Z, Szelei J, Lacoste MC, Li Y, Gariepy S, Raymond P, Allaire M, Nabi IR, Tijssen P.** 2001. A viral phospholipase A2 is required for parvovirus infectivity. Dev Cell **1:**291–302. http://dx.doi.org/10.1016/S1534-5807(01)00031-4.
69. **Canaan S, Zadori Z, Ghomashchi F, Bollinger J, Sadilek M, Moreau ME, Tijssen P, Gelb MH.** 2004. Interfacial enzymology of parvovirus phospholipases A2. J Biol Chem **279:**14502–14508. http://dx.doi.org/10.1074/jbc.M312630200.
70. **Mitchell KJ, Pinton P, Varadi A, Tacchetti C, Ainscow EK, Pozzan T, Rizzuto R, Rutter GA.** 2001. Dense core secretory vesicles revealed as a dynamic Ca(2+) store in neuroendocrine cells with a vesicle-associated membrane protein aequorin chimaera. J Cell Biol **155:**41–51. http://dx.doi.org/10.1083/jcb.200103145.
71. **Spooner RA, Smith DC, Easton AJ, Roberts LM, Lord JM.** 2006. Retrograde transport pathways utilised by viruses and protein toxins. Virol J **3:**26. http://dx.doi.org/10.1186/1743-422X-3-26.
72. **Lauvrak SU, Torgersen ML, Sandvig K.** 2004. Efficient endosome-to-Golgi transport of Shiga toxin is dependent on dynamin and clathrin. J Cell Sci **117:**2321–2331. http://dx.doi.org/10.1242/jcs.01081.
73. **Nichols BJ.** 2002. A distinct class of endosome mediates clathrin-independent endocytosis to the Golgi complex. Nat Cell Biol **4:**374–378. http://dx.doi.org/10.1038/ncb787.
74. **Kotchey NM, Adachi K, Zahid M, Inagaki K, Charan R, Parker RS, Nakai H.** 2011. A potential role of distinctively delayed blood clearance of recombinant adeno-associated virus serotype 9 in robust cardiac transduction. Mol Ther **19:**1079–1089. http://dx.doi.org/10.1038/mt.2011.3.
75. **Qiao CP, Yuan ZH, Li JB, Tang RH, Li J, Xiao X.** 2012. Single tyrosine mutation in AAV8 and AAV9 capsids is insufficient to enhance gene delivery to skeletal muscle and heart. Hum Gene Ther Methods **23:**29–37. http://dx.doi.org/10.1089/hgtb.2011.229.
76. **Mellman I.** 1996. Endocytosis and molecular sorting. Annu Rev Cell Dev Biol **12:**575–625. http://dx.doi.org/10.1146/annurev.cellbio.12.1.575.
77. **Lundmark R, Doherty GJ, Howes MT, Cortese K, Vallis Y, Parton RG, McMahon HT.** 2008. The GTPase-Activating Protein GRAF1 Regulates the CLIC/GEEC Endocytic Pathway. Curr Biol **18:**1802–1808. http://dx.doi.org/10.1016/j.cub.2008.10.044.